DOI: 10.19884/j.1672-5220.202408002

A Hybrid Simulation-Experimental Method for Deriving Equivalent Dynamic Parameters of O-Ring Support Systems

LIU Yi[1], YE He[1,2], ZHANG Lingfeng[1], LI Shujia[1,3], CHEN Ge[1,3], WANG Yongxing[1,3*]
1. College of Mechanical Engineering, Donghua University, Shanghai 201620, China
2. China Textile Machinery Association, Beijing 100028, China
3. Engineering Research Center of Advanced Textile Machinery, Ministry of Education, Shanghai 201620, China

Abstract: The high-speed winding spindle employs a flexible support system incorporating rubber O-rings. By precisely configuring the structural parameters and the number of the O-rings, the spindle can stably surpass its critical speed points and maintain operational stability across the entire working speed range. However, the support stiffness and damping of rubber O-rings exhibit significant nonlinear frequency dependence. Conventional experimental methods for deriving equivalent stiffness and damping, based on the principle of the forced non-resonance method, require fabricating custom setups for each O-ring specification and conducting vibration tests at varying frequencies, resulting in low efficiency and high costs. This study proposes a hybrid simulation-experimental method for dynamic parameter identification. Firstly, the frequency-dependent dynamic parameters of a specific O-ring support system are experimentally obtained. Subsequently, a corresponding parametric finite element model is established to simulate and solve the equivalent elastic modulus and equivalent stiffness-damping coefficient of this O-ring support system. Ultimately, after iterative simulation, the simulated and experimental results achieve a 99.7% agreement. The parametric finite element model developed herein can directly simulate and inversely estimate frequency-dependent dynamic parameters for O-rings of different specifications but identical elastic modulus.

Keywords: O-ring; equivalent dynamic parameter; forced non-resonance method; inverse parameter estimation; dynamic simulation
CLC number: TQ340.5 **Document code**: A
Article ID: 1672-5220(2025)04-0425-10

Open Science Identity (OSID)

0 Introduction

The high-speed winding machine is an essential piece of equipment in polyester and nylon filament production lines, usually with winding speeds of up to 3 500 m/min for pre-oriented yarn (POY) and 5 500 m/min for fully drawn yarn (FDY). To accommodate these high speeds, the spindle operates within a wide range of rotational speeds: 0 to 9 000 r/min for POY and 0 to 12 500 r/min for FDY. To improve production efficiency, the spindle features a large length-diameter ratio and a thin-wall structure, accommodating up to 16 filament packages.

To maintain a constant winding linear speed as the package diameter increases, the rotational speed of the spindle needs to be proportionally reduced. To achieve this, precise control over the equivalent dynamic parameters of the flexible support system is essential. By optimizing the configuration of O-rings, the system can effectively suppress vibrations and ensure smooth operation as the spindle passes through its critical speed points with an increasing mass of packages. The structure of the winding spindle is shown in Fig. 1[1]. The bushing and supporting arm are connected by O-rings. The bushing is designed with multiple installation ports for O-rings, allowing the dynamic performance of the entire flexible support system to be adjusted by varying the number of O-rings.

The damping of the flexible support system is mainly provided by the rubber O-ring (hereafter abbreviated as the O-ring). The stiffness of the flexible support system is determined by the rolling bearing and the O-ring in series. Due to the fact that the stiffness of the bearings does not have frequency-varying characteristics and is constant, once the stiffness of the O-ring is known, the stiffness of the entire support system can be obtained. Therefore, this paper mainly studies the equivalent dynamic parameters of the O-ring. The corresponding dynamic model is shown in Fig. 2, where k_r is the equivalent stiffness; c_r is the equivalent damping of the O-ring.

Received date: 2024-08-05
Foundation items: National Key R&D Program of China (No. 2017YFB1304000); Fundamental Research Funds for the Central Universities, China (No. 2232023G-05-1)
* Correspondence should be addressed to WANG Yongxing, email: wangyx@dhu.edu.cn
Citation: LIU Y, YE H, ZHANG L F, et al. A hybrid simulation-experimental method for deriving equivalent dynamic parameters of O-ring support systems[J]. *Journal of Donghua University (English Edition)*, 2025, 42(4): 425-434.

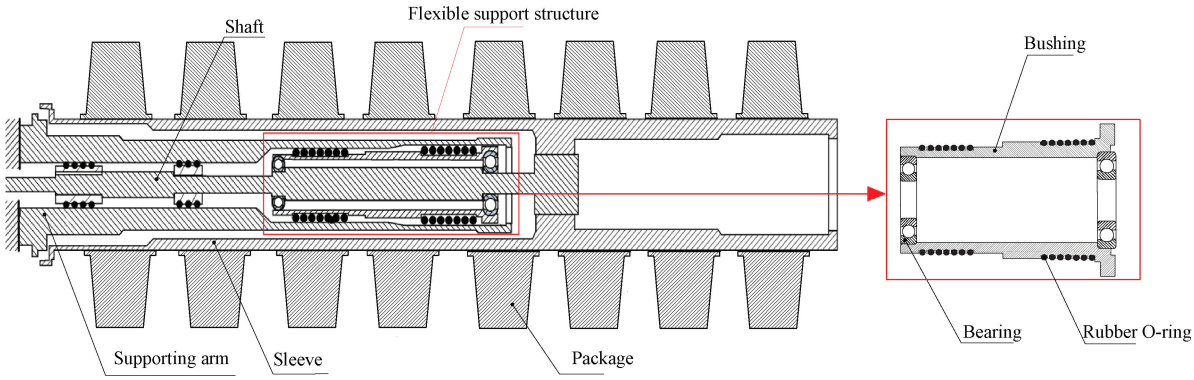

Fig. 1 Spindle structure

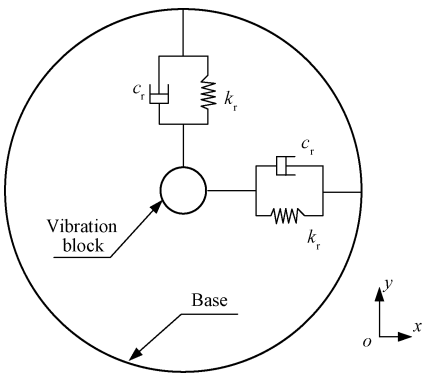

Fig. 2 Dynamic model of flexible support system

The effectiveness of the O-ring in mitigating high-frequency vibrations has been widely recognized in various fields, such as automotive engine suspensions, combustion instability of solid propellant rocket engines[2], and ultrasonic testing of piping systems with a flange gasket[3]. In the flexible support system of the spindle, the O-ring can reduce the critical speed and enable the spindle to pass through the critical speed points with an acceptable small amplitude during the winding process.

The research on the characteristics of rubber focuses on the influence of excitation frequency, temperature, rubber size, cross-sectional diameter, and extrusion on the stiffness and damping characteristics of various rubber materials[4-7]. Due to the complex characteristics of rubber, current research on equivalent dynamic parameters of rubber is mainly conducted through experiments. Wang et al.[8] and Sun et al.[9] used experimental tests and employed nonlinear least squares to obtain the relationship between the equivalent dynamic parameters of the flexible support system and frequency.

In the current technological landscape, simulation is a mainstream method for dynamics research due to its low cost, high efficiency and the ability to model complex scenarios[10-11], while experiments remain vital for validation. However, the accuracy of rubber equivalent material parameters affects the simulation results. A common approach to characterizing the performance of rubber materials is to use constitutive models such as Mooney-Rivlin[12], Ogden[13] and Yeoh[14], which establish stress-strain relationships for hyperelastic behavior. However, these models are primarily suited for static conditions and fail to accurately capture dynamic properties, as the performance of the O-ring depends on compression, temperature and frequency[15]. Some scholars added viscoelastic analysis to address the shortcomings of the above constitutive models in frequency conversion situations[16], and compared simulation and experimental results to derive empirical model parameters. Sim et al.[17] proposed a method for experimentally obtaining rubber equivalent material parameters, but the formula used in this method has requirements for the shape of the rubber.

This paper presents a hybrid simulation-experimental method for deriving the equivalent dynamic parameters. The overall process of this paper is shown in Fig. 3.

Firstly, the dynamic parameters (equivalent stiffness k_r and equivalent damping c_r) of a specific O-ring support system are derived through experiments. Then, a corresponding parametric finite element model is established to simulate and calculate the equivalent dynamic parameters (k_r^* and c_r^*) of this O-ring support system. The iterative method entails repeatedly adjusting the rubber material parameters (equivalent elastic modulus E^* and equivalent stiffness-damping coefficient β^*) within a defined range through simulations until the simulated parameters (k_r^* and c_r^*) converge to the experimental parameters (k_r and c_r), thereby reducing the error e to an acceptable tolerance. As a result, the simulated equivalent dynamic parameters (k_r^* and c_r^*) and the O-ring material parameters (E^* and β^*) are identified. Advantageously, by using the characterized O-ring material parameters (E^* and β^*), the equivalent dynamic parameters (k_r^* and c_r^*) of the O-ring with the same material but different O-ring specifications can be quickly derived just by simulation.

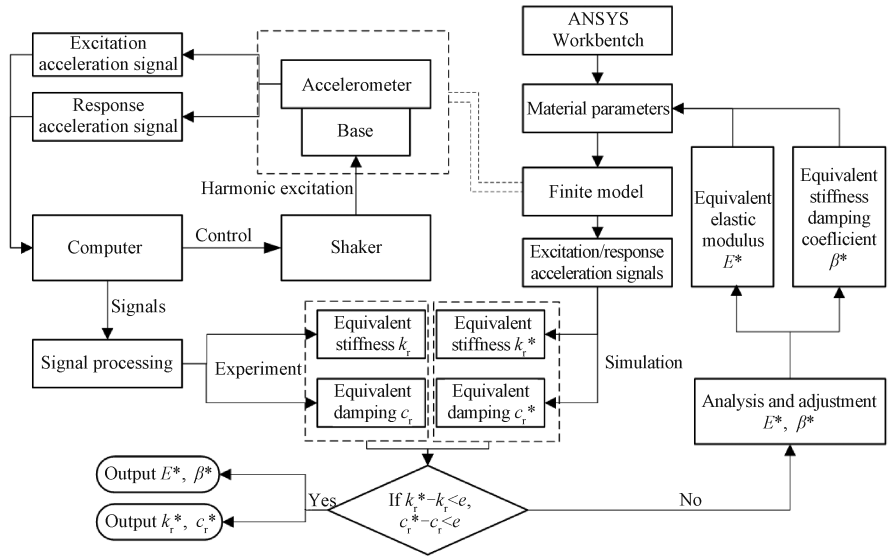

Fig. 3 Flowchart of hybrid simulation-experimental method

1 Dynamic Testing Method

The dynamic testing methods commonly used include the free vibration method[18], the forced resonance method[19], and the forced non-resonance method[20]. The forced non-resonance method identifies equivalent dynamic parameters by applying external loads to the support system's base (not directly connected to the vibration block). This approach avoids natural frequency excitation, which would cause undesirable resonance effects. By operating in non-resonant-frequency ranges of the frequency domain, the method safely measures the support system's dynamic characteristics.

1.1 Principle of single-degree-of-freedom forced non-resonance method

The principle of the single-degree-of-freedom forced non-resonance method for deriving relevant equivalent dynamic parameters is illustrated in Fig. 4. The Newton's equation of motion describing the vibration block under the action of external load can be written as

$$m\ddot{x}_1 + c_r(\omega)(\dot{x}_1 - \dot{x}_0) + k_r(\omega)(x_1 - x_0) = 0, \quad (1)$$

where m is the mass of the vibration block; x_0 is the excitation displacement of the base; x_1 is the response displacement of the vibration block; $\dot{x}_0$ is the excitation velocity of the base; $\dot{x}_1$ is the response velocity of the vibration block; $\ddot{x}_1$ is the response acceleration of the vibration block; $k_r(\omega)$ and $c_r(\omega)$ are the equivalent support stiffness and damping of the O-ring, respectively, and both of them are functions of angular frequency ω.

It can be assumed that the simple harmonic excitation displacement x_0 acting on the base, and the response displacement x_1 can be written in the complex exponential function:

$$\begin{cases} x_0 = a_0 e^{i\omega t}, \\ x_1 = a_1(\omega) e^{i(\omega t - \varphi(\omega))}, \end{cases} \quad (2)$$

where a_0 is the excitation amplitude of the base in angular frequency ω; $a_1(\omega)$ is the response amplitude of the base in angular frequency ω; t is the time.

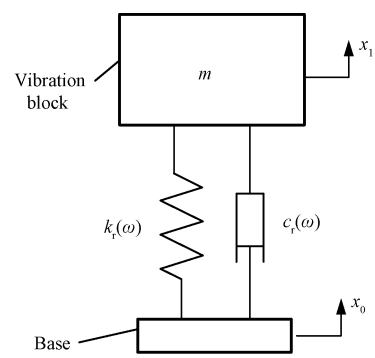

Fig. 4 Single-degree-of-freedom dynamic model

By calculating individually the first-order and second-order derivatives of the excitation and response in Eq. (2) with respect to the time t, the velocity amplitude v_0 and acceleration amplitude u_0 of the base, as well as the corresponding response velocity $v_1(\omega)$ and acceleration amplitude $u_1(\omega)$ of the vibration block, are obtained. The amplitude ratio $\alpha(\omega)$ can be calculated as

$$\alpha(\omega) = \frac{a_1(\omega)}{a_0} = \frac{v_1(\omega)}{v_0} = \frac{u_1(\omega)}{u_0}. \quad (3)$$

By substituting Eq. (2) into Eq. (1) and setting the real part and imaginary part to be 0, respectively, the equivalent dynamic parameters can be obtained as

$$\begin{cases} k_r(\omega) = \dfrac{m\omega^2[\alpha^2(\omega) - \alpha(\omega)\cos(\varphi(\omega))]}{\alpha^2(\omega) - 2\alpha(\omega)\cos(\varphi(\omega)) + 1}, \\ c_r(\omega) = \dfrac{m\omega\alpha(\omega)\sin(\varphi(\omega))}{\alpha^2(\omega) - 2\alpha(\omega)\cos(\varphi(\omega)) + 1}, \end{cases} \tag{4}$$

where $\varphi(\omega)$ is the phase difference of the two signals. $\alpha(\omega)$ and $\varphi(\omega)$ are obtained through the corresponding finite element model simulation solution according to Eq. (1), based on the single-degree-of-freedom forced non-resonance method.

Therefore, when the vibration block mass m, the excitation angular frequency ω, the amplitude ratio $\alpha(\omega)$ and the phase difference $\varphi(\omega)$ of the two accelerations are known. The equivalent support stiffness $k_r(\omega)$ and equivalent support damping $c_r(\omega)$ of the single-degree-of-freedom system can be calculated by Eq. (4).

1.2 Conditions for single-degree-of-freedom forced non-resonance method

The external excitation of the base should be kept far away from the natural frequency of the experimental device to avoid resonance; otherwise, it could cause large errors in the experimental and simulation results. Therefore, to determine the excitation frequency range which can be applied under a certain natural frequency, a numerical analysis is performed to stabilize the experimental and simulation results[8].

From Eq. (4), the expression equations of the amplitude ratio $\alpha(\omega)$ and the phase difference $\varphi(\omega)$ can be obtained as follows:

$$\begin{cases} \alpha(\omega) = \left[\dfrac{k_r^2(\omega) + c_r^2(\omega)\omega^2}{k_r(\omega) - m\omega^2 + c_r^2(\omega)\omega^2}\right]^{\frac{1}{2}} = \\ \qquad \left[\dfrac{1 + (2\xi\gamma)^2}{(1-\gamma^2)^2 + (2\xi\gamma)^2}\right]^{\frac{1}{2}}, \\ \varphi(\omega) = \tan\left[\dfrac{2\xi\gamma^3}{1 - \gamma^2 + (2\xi\gamma)^2}\right], \end{cases} \tag{5}$$

where ξ is the damping ratio of the base, and $\xi = c_r(\omega)/[2\sqrt{mk_r(\omega)}]$; γ is the frequency ratio, and $\gamma = \dfrac{\omega}{\omega_n}$; ω_n is the natural angular frequency and $\omega_n = \sqrt{k_r(\omega)/m}$.

The changes of $\alpha(\omega)$ and $\varphi(\omega)$ with γ and ξ are shown in Fig. 5 and Fig. 6.

It can be seen that when $0.707 < \gamma < 1.350$, the change of $\alpha(\omega)$ is influenced by frequency ratio γ greatly, thus γ should meet $\gamma \leqslant 0.707$ or $\gamma \geqslant 1.350$.

When $\gamma \leqslant 0.707$, the amplitude ratio $\alpha(\omega) > 1$, and $\cos(\varphi(\omega)) \approx 1$. The stiffness calculation expression $k_r(\omega)$ in Eq. (4) at this time can be simplified as[21]

$$k_r(\omega) = m\omega^2\vartheta(\omega), \tag{6}$$

where $\vartheta(\omega) = \dfrac{\alpha^2(\omega) - \alpha(\omega)}{\alpha^2(\omega) - 2\alpha(\omega) + 1} = \dfrac{\alpha(\omega)}{\alpha(\omega) - 1}$.

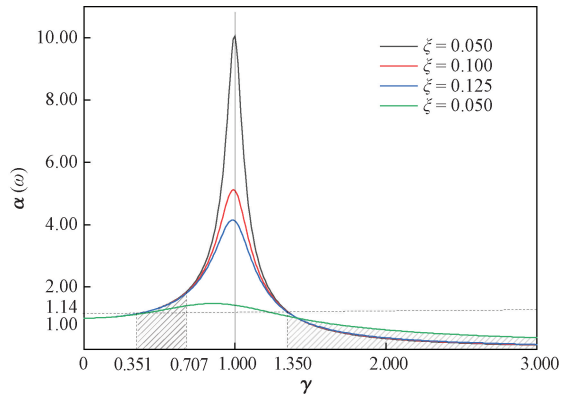

Fig. 5 Variation curves of $\alpha(\omega)$ with frequency ratio γ and damping ratio ξ

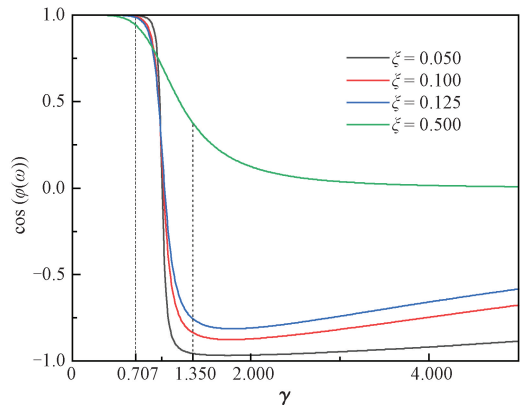

Fig. 6 Variation curves of $\cos(\varphi(\omega))$ with frequency ratio γ and damping ratio ξ

The changes of $\vartheta(\omega)$ with $\alpha(\omega)$ are shown in Fig. 7.

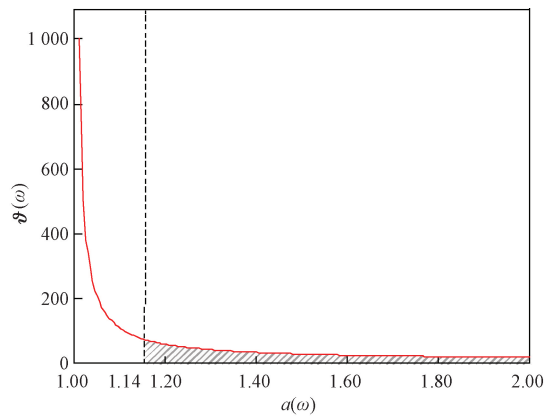

Fig. 7 Variation curve of $\vartheta(\omega)$ with $\alpha(\omega)$

Figure 7 shows that when $1.00 < \alpha(\omega) < 1.14$, $\alpha(\omega)$ has a great impact on the value of $\vartheta(\omega)$, and a small change of $\alpha(\omega)$ causes a large fluctuation to $\vartheta(\omega)$. This has a significant impact on the accuracy of the testing and simulation results by the forced non-resonance method. To ensure the accuracy of the testing and simulation results, the value of $\vartheta(\omega)$ must not be too large, and thus $\alpha(\omega)$ needs to satisfy $\alpha(\omega) \geqslant 1.14$. From Fig. 5, when $\alpha(\omega) \geqslant 1.14$, the frequency ratio γ

needs to satisfy $\gamma \geqslant 0.351$.

Therefore, based on the principle of the single-degree-of-freedom forced non-resonance method, from Fig. 5, the excitation frequency should meet

$$\begin{cases} 0.351\omega_n \leqslant \omega \leqslant 0.707\omega_n, \\ \omega \geqslant 1.350\omega_n. \end{cases} \tag{7}$$

2 Experiment and simulation

2.1 Experiment

According to the polyester filament winding process, the winding linear speed of the package needs to be kept constant during the whole winding process. The working rotational speed of a spindle is 0–16 000 r/min and the working frequency is 0–266.7 Hz. Because the frequency-dependent characteristics of the flexible support are not obvious in the low-frequency range, the test frequency range in this paper is set to 80–300 Hz.

The actual experimental test device is shown in Fig. 8. Keeping consistency in structure and the O-ring parameters between experiment and simulation, the necessary parameters for following simulation are obtained through experimental testing.

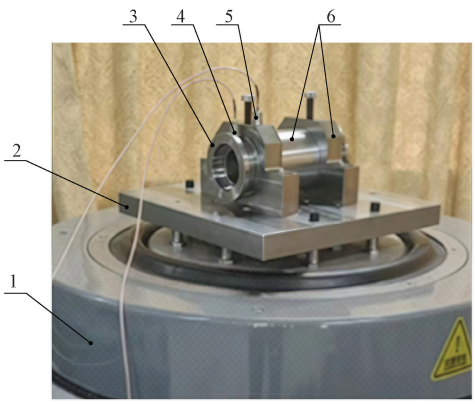

1—excitation device; 2—base plate; 3—vibration block; 4—acceleration sensor Ⅰ (response); 5—acceleration sensor Ⅱ (excitation); 6—base.

Fig. 8 Experimental testing device

The computer can provide front-end control through LMS SCADAS (data acquisition hardware) and the acceleration model is obtained by the acceleration sensor on the vibration device. The acceleration signal obtained from the experiment has spikes, which require filtering and correlation analysis to obtain the amplitude and phase difference of the excitation acceleration and response acceleration, and then the equivalent stiffness and equivalent damping are obtained.

Due to the difficulty of changing the mass of the vibration block in experiments, changing the number of the O-rings can more quickly alter the natural frequency of the experimental setup in this situation. The sweep frequency curve of the experimental testing device can obtain experiment results under different numbers of the O-rings. The first-order natural frequency of the testing system and the experimental testing range based on the forced non-resonance method conditions are illustrated in Fig. 9.

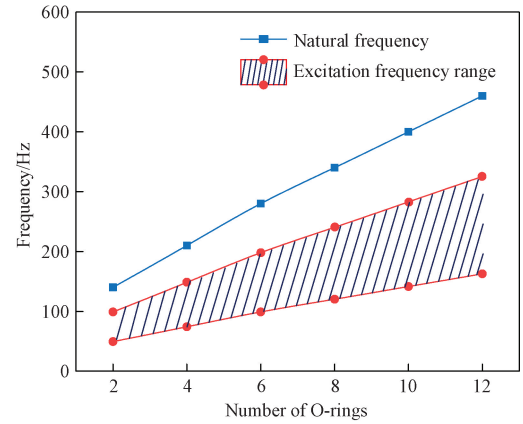

Fig. 9 Support system excitation frequency range

2.2 Simulation

2.2.1 Model

The structures (e.g., grooves and screws) of the experimental testing device are simplified in the finite element model. By extracting the key structures of the device, the finite element model of the O-ring base structure is shown in Fig. 10. To save time, the model is cut along the *XOY* plane and set to be symmetrical. By calculating half of the model, the corresponding results can be obtained.

The main structure of the finite element model includes the base, the O-rings that play a supporting role, and the vibration block in the middle. In the experimental configuration, the O-rings are pre-compressed within the device to provide structural support.

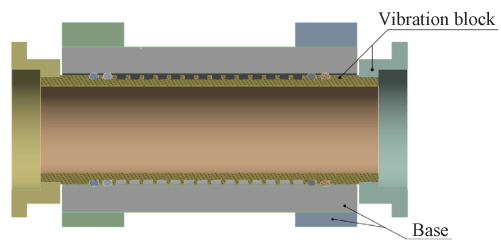

Fig. 10 Finite element model

2.2.2 Material parameters

When performing simulation by using the finite element models in ANSYS Workbench, material parameters need to be input. The equivalent elastic modulus E^* and equivalent stiffness-damping coefficient β^* of the O-ring are taken as unknown variables.

Compared with the O-ring, the base and vibration block can be regarded as a rigid body, and the parameters of the O-ring material are shown in Table 1.

Table 1 O-ring material parameters

Material	Poisson's ratio	Hardness/IRHD	Outer diameter/mm	Cross-sectional diameter/mm	Compression amount
Nitrile butadiene rubber	0.48	64	50	4	20%

Notes: IRHD means international rubber hardness degree; compression amount is defined as the reduction in cross-section diameter.

2.2.3 Contact settings

The bearing seat sleeve and the O-ring mounting sleeve are connected by an interference fit. The support frame and the experimental fixing sleeve are connected by a clearance fit and fastened by bolts. The mounting sleeve is connected to the experimental fixing sleeve through the O-ring in the groove.

The interference fits have little effect on the mode and can be simplified as consolidation.

The connections between the O-ring and the mounting sleeve and the experimental fixing sleeve are set to no-separation contact. When two models with different hardness materials are set in contact, the side with lower hardness is set as the contact surface, and the side with higher hardness is set as the target surface. Therefore, the O-ring is set as the contact surface, and the experimental fixing sleeve and the O-ring mounting sleeve are set as the target surface.

2.2.4 Meshing

Due to the regular shape of the model, the O-ring mounting sleeve, the experimental fixing sleeve and the bearing housing sleeve are meshed with a 5 mm hexahedral grid, and due to the small structure in the O-ring mounting sleeve, an adaptive grid is used to refine the mesh at appropriate positions.

Since the O-rings have a great influence on the results of the system study, they are more finely meshed. The mesh characteristics of the O-ring are set to linear reduction integral units, which are represented in ANSYS Workbench as C3D8R, and the mesh size for the O-ring is 1 mm, as shown in Fig. 11.

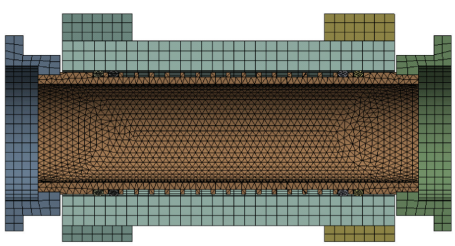

Fig. 11 Model meshing

2.2.5 Boundary conditions and loading settings

The excitation device performs simple harmonic vibration in the vertical direction, applying simple harmonic excitation displacement x_0 ($x_0 = a_0\sin(\omega t)$) to the bottom of the support frame, where $a_0 = 0.05$ mm. Five degrees of freedom are constrained on the support frame and the vibration block mass, retaining only the degree of freedom in the vertical direction.

The equivalent dynamic parameters of the O-ring can be derived at the working frequency by changing the size of the vibration mass in the finite element model. After adjusting the vibration mass in the simulation, the natural frequency of the system and the corresponding test frequency range are shown in Table 2.

Table 2 Natural frequency and corresponding test frequency range after adjusting vibration block mass

Number	Vibration block mass m/kg	Natural frequency f_n/Hz	Test frequency f/Hz
1	13.01	150	80–100
2	3.25	300	120–200
3	0.97	550	200–300

By using transient structural analysis in ANSYS, the initial frequency is set as 80 Hz. The results are recorded and repeated every 20 Hz to obtain the corresponding signal in a frequency range of 80 to 300 Hz.

3 Results and Discussion

Taking a four-O-ring support as an example, $a_0 = 0.05$ mm, $f = 140$ Hz, a simple harmonic excitation displacement x_0 ($x_0 = 0.05\sin(2\pi \times 140t)$) is applied to the bottom of the support frame, and the acceleration load on the plane is $\ddot{x}_0 = -38\,688.8\sin(2\pi \times 140t)$. The acceleration on the plane obtained by simulation is 39 023.5 mm/s^2. The error with the theoretical analysis result is only 0.86%. This shows that the boundary conditions set in this paper according to the excitation device are reasonable and efficient. There is a certain proportional relationship between equivalent material parameters and equivalent dynamic parameters, which can quickly lock in the fitting range of equivalent material parameters.

When the frequency is 140 Hz and the equivalent elastic modulus E^* is set to 2×10^7 Pa, c_r increases with the increase of β^* (Fig. 12).

Similarly, when maintaining $\beta^* = 0.000\,3$ s at the same frequency and varying only the equivalent elastic modulus E^*, the results demonstrate: 1) a linear increase in equivalent stiffness k_r with E^* (Fig. 13(a)); 2) a linear increase in the equivalent damping coefficient c_r with E^* (Fig. 13(b)).

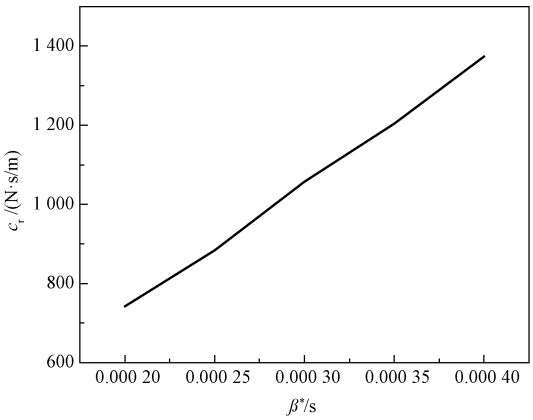

Fig. 12 Relationship between c_r and β^*

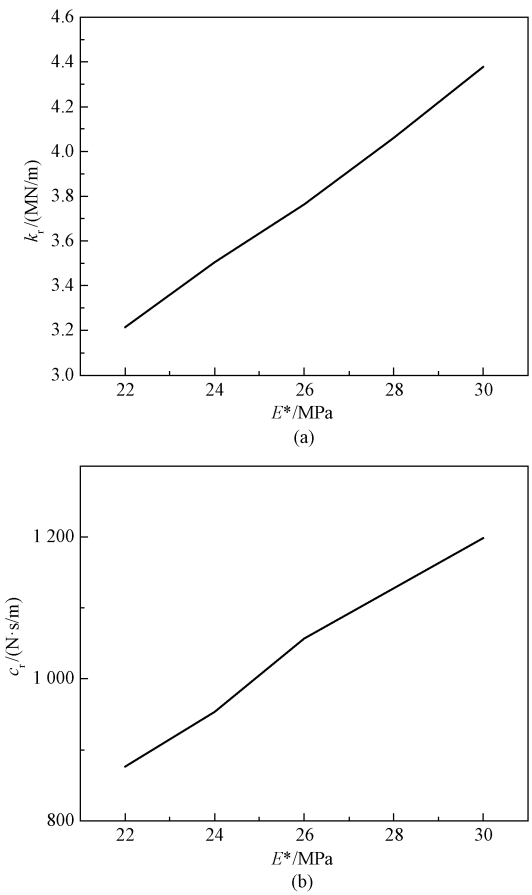

Fig. 13 Relationship between equivalent dynamic parameters and E^*: (a) k_r vs. E^*; (b) c_r vs. E^*

The parametric analysis reveals three fundamental linear correlations governing the system's dynamic behavior: 1) $\beta^* \propto c_r$; 2) $E^* \propto k_r$; 3) $E^* \propto c_r$. Since β^* does not show a linear correlation with k_r, the equivalent material parameter range corresponding to the equivalent dynamic parameters can be obtained based on the above three correlations, and the final parameter results that meet the needs can be derived through small-scale adjustments.

Experimental results show that the equivalent stiffness and damping are proportional to the number of O-rings. We therefore normalized these parameters by O-ring quantity to compare their frequency-dependent behaviors. The relationship of the results between experiment and simulation is shown in Fig. 14.

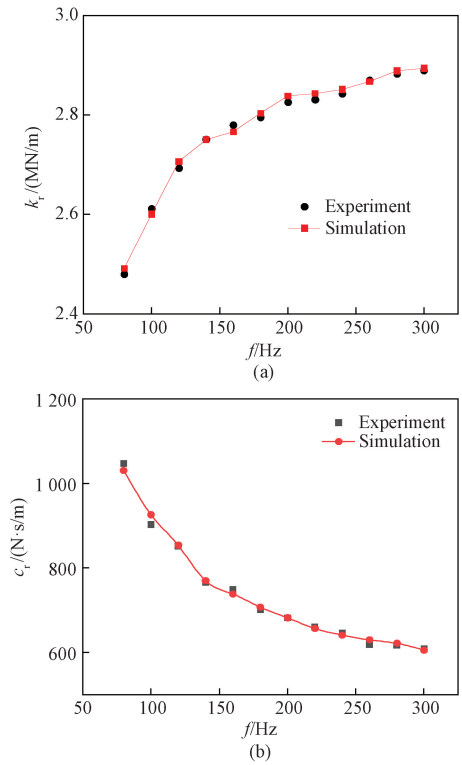

Fig. 14 Relationship between equivalent dynamic parameters and f: (a) k_r vs. f; (b) c_r vs. f

When obtaining the experimental and simulation fitting curve with an error of 0.3% in Fig. 14, the corresponding equivalent material parameters are shown in Fig. 15.

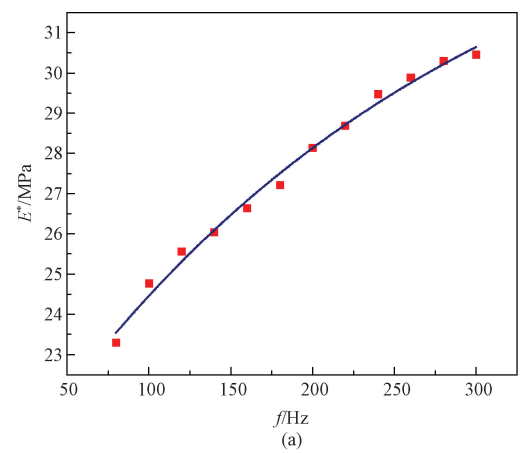

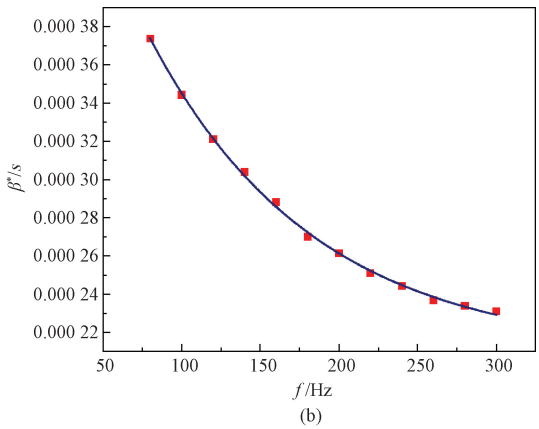

Fig. 15 Relationship between equivalent material parameters and f: (a) E^* vs. f; (b) β^* vs. f

The derived material parameter curve is fitted nonlinearly. The corresponding result is

$$\begin{cases} E^*(f) = g_0 e^{-f/h_0} + k_0, \\ \beta^*(f) = g_1 e^{-f/h_1} + k_1, \end{cases} \tag{8}$$

where g_0, h_0 and k_0 are the amplitude coefficient, decay frequency and asymptotic elastic modulus for the elastic modulus E^*, respectively; g_1, h_1 and k_1 are the amplitude coefficient, decay frequency and asymptotic damping coefficient for the damping coefficient β^*, respectively.

The corresponding parameters are shown in Table 3.

Applying the equivalent material parameters to the O-ring support systems of the same material but different O-ring sizes, their frequency-dependent equivalent dynamic parameters can be derived just using the dynamic simulation. The O-ring specification is set in Table 4.

Table 3 Fit parameters

Parameter	g_0	h_0	k_0	g_1	h_1	k_1
Value	-1.701×10^7	2.540×10^2	3.611×10^7	3.543×10^{-4}	1.045×10^2	2.090×10^{-4}

Table 4 Parameters of O-rings with different sizes

Number	Outer diameter/mm	Cross-sectional diameter/mm	Sample name
1	50.0	4.0	50×4
2	47.0	4.0	47×4
3	46.0	3.5	46×3.5

When the size of an O-ring is modified, its support system undergoes proportional changes in both geometry and mass properties. Although these structural variations may appear minor, they significantly alter the system's dynamic response. Crucially, the fundamental equivalent material parameters remain invariant across sizes for a given compound. Therefore, the equivalent material parameters can be directly input into the finite element model to derive its equivalent dynamic parameters, as shown in Fig. 16.

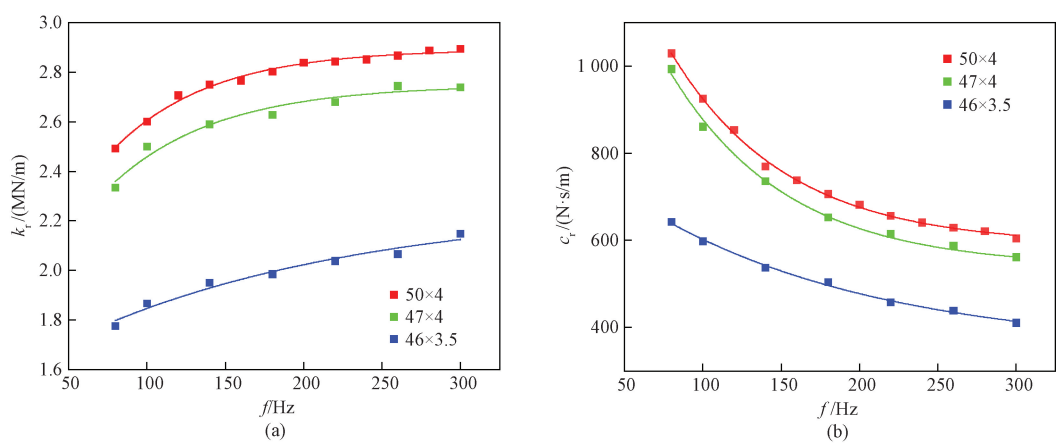

Fig. 16 Equivalent dynamic parameter curves of different O-rings: (a) k_r vs. f; (b) c_r vs. f

Analyses of the equivalent dynamic parameters reveal consistent scaling behavior across different O-ring sizes, enabling performance prediction with minimal experimental data points. When the size of the O-ring decreases, the volume of the material involved in elastic deformation decreases, and the overall stiffness decreases. At the same time, the scale of the molecular chain mesh inside the O-ring decreases, the ability to dissipate energy weakens, and its loss factor also decreases.

4 Conclusions

A dynamic equivalent material parameter deriving method that combines experimental testing and numerical simulation for O-rings in the flexible support system is

proposed in this study. Based on the forced non-resonance principle, the frequency range far from the resonance region is obtained. The corresponding frequency ranges are obtained by changing the number of O-rings in the experiment, and the corresponding frequency range in the simulation is directly obtained by changing the mass of the vibration block.

Based on the relationship between equivalent material parameters and equivalent dynamic parameters, the equivalent material parameters of the O-ring can be dynamically adjusted to obtain corresponding equivalent material parameters with excellent fitting to the dynamic parameter results at different frequencies. These equivalent material parameters correspond to the actual experimental results and can accurately describe the material nonlinearity and frequency variability. The approach proposed in this study enables the direct application of the calibrated equivalent material parameters to simulate O-ring support systems of varying sizes, as long as material consistency is maintained. By adjusting the O-ring size, the corresponding equivalent dynamic parameters can be derived just by using dynamic simulation, significantly reducing research and development costs and cycles.

References

[1] LI Z, GAN X H, LIU G Z, et al. Experiment and analysis of dynamic parameters of elastomer O-ring support of winding machine spindle[J]. *Journal of Donghua University (Natural Science Edition)*, 2018, 44(5):779-786. (in Chinese)

[2] MONTESANO J, BEHDINAN K, GREATRIX D R, et al. Internal chamber modeling of a solid rocket motor: effects of coupled structural and acoustic oscillations on combustion[J]. *Journal of Sound and Vibration*, 2008, 311(1/2): 20-38.

[3] CHO H, ROKHLIN S I. Interface wave propagation and edge conversion at a low stiffness interphase layer between two solids: a numerical study[J]. *Ultrasonics*, 2015, 62: 213-222.

[4] TOMIOKA J, MIYANAGA N. Measurement of dynamic properties of O-rings and stability threshold of flexibly supported herringbone grooved aerodynamic journal bearings [J]. *Tribology Online*, 2008, 3(7): 366-369.

[5] AL-BENDER F, COLOMBO F, REYNAERTS D, et al. Dynamic characterization of rubber O-rings: squeeze and size effects[J]. *Advances in Tribology*, 2017, 2017(1): 2509879.

[6] GREEN I, ETSION I. Pressure and squeeze effects on the dynamic characteristics of elastomer O-rings under small reciprocating motion[J]. *Journal of Tribology*, 1986, 108(3): 439-444.

[7] BÄTTIG P, SCHIFFMANN J. Data-driven model for the dynamic characteristics of O-rings for gas bearing supported rotors[J]. *Journal of Applied Mechanics*, 2019, 86(8): 081003.

[8] WANG Y X, ZHANG L J, HOU X, et al. A dynamic modeling approach for the winding spindle during start-up with a coupled flexible support system[J]. *Textile Research Journal*, 2020, 90(7/8): 757-775.

[9] SUN D W, CHEN Z G, ZHANG G Y, et al. Modeling and parameter identification of amplitude- and frequency-dependent rubber isolator[J]. *Journal of Central South University*, 2011, 18(3): 672-678.

[10] TANG L, ZUN K. Hardware-in-the-loop simulation system based on Unity3D for winding machine[J]. *Journal of Donghua University (English Edition)*, 2024, 41(3): 298-307.

[11] ZHU C Y, CAO H Y, DING G F, et al. Comparative simulation study of active sound absorption based on piezoelectric materials[J]. *Journal of Donghua University (English Edition)*, 2024, 41(3): 308-314.

[12] SZABÓ G, VÁRADII K. Large strain viscoelastic material model for deformation, stress and strain analysis of O-rings[J]. *Periodica Polytechnica Mechanical Engineering*, 2018, 62(2): 148-157.

[13] OGDEN R W. Non-linear elastic deformations[M]. Chelmsford: Courier Corporation, 1997.

[14] YANES E, PUGNO N M, RAMIER J, et al. Characterising the friction coefficient between rubber O-rings and a rigid surface under extreme pressures[J]. *Polymer Testing*, 2021, 104: 107378.

[15] SHOYAMA T, FUJIMOTO K. Direct measurement of high-frequency viscoelastic properties of pre-deformed rubber[J]. *Polymer Testing*, 2018, 67: 399-408.

[16] LEE H S, SHIN J K, MSOLLI S, et al. Prediction of the dynamic equivalent stiffness for a rubber bushing using the finite element method and empirical modeling [J]. *International Journal of Mechanics and Materials in Design*, 2019, 15(1): 77-91.

[17] SIM S, KIM K J. A method to determine the complex modulus and Poisson's ratio of viscoelastic materials for FEM applications[J]. *Journal of Sound and Vibration*, 1990, 141(1): 71-82.

[18] FELDMAN M. Non-linear system vibration analysis using Hilbert transform: I. Free vibration analysis method 'Freevib'[J]. *Mechanical Systems and Signal Processing*, 1994, 8(2): 119-127.

[19] LI R, FAN G S, OUYANG X, et al. Dynamic mechanical behaviors of epoxy resin/hollow polymeric microsphere composite foams under forced non-resonance and forced resonance[J]. *Composites and Advanced Materials*, 2021, 30:

26349833211008195.
[20] OYADIJI S O, TOMLINSON G R. Determination of the complex moduli of viscoelastic structural elements by resonance and non-resonance methods [J]. *Journal of Sound and Vibration*, 1985, 101(3): 277-298.
[21] THORBY D. Structural dynamics and vibration in practice: an engineering handbook [M]. Oxford: Butterworth-Heinemann, 2008.

仿真和实验结合获取含O型圈支承系统动力学参数方法

刘　怡[1], 叶　贺[1,2], 张凌风[1], 李姝佳[1,3], 陈　革[1,3], 王永兴[1,3*]
1. 东华大学 机械工程学院, 上海 201620
2. 中国纺织机械协会, 北京 100028
3. 纺织装备教育部工程研究中心, 上海 201620

摘　要: 高速卷绕锭轴采用含O型橡胶圈的柔性支承系统, 通过精确配置O型橡胶圈结构参数和数量使其稳定越过临界转速点, 并确保锭轴在全工况转速范围内稳定运转。O型橡胶圈的支承刚度、阻尼系数具有显著的非线性频变特性, 目前基于强迫非共振法求取等效刚度和阻尼的实验测试方法需要针对不同规格橡胶圈制作不同规格的实验装置, 进行不同频率下的振动响应测试, 效率低且成本高。该文提出一种综合仿真和实验的动力学参数识别方法。首先通过实验获取某一规格O型圈支承系统的具有频变特性的等效动力学参数。然后建立对应参数化有限元仿真模型, 采用动力学仿真方法反求该支承系统等效弹性模量和等效刚度阻尼系数。经过仿真计算和参数迭代, 仿真和实验获得的等效动力学参数吻合度高达99.7%。该文开发的参数化有限元模型可以直接模拟和估算不同规格但弹性模量相同的O型圈支承系统的频变动力学参数。

关键词: O型圈; 等效动力学参数; 强迫非共振法; 参数反求; 动力学仿真